Efficient Local Classical Shadow Tomography with Number Conservation

Sumner N. Hearth, Michael O. Flynn, Anushya Chandran, and Chris R. Laumann
Department of Physics, Boston University, 590 Commonwealth Avenue, Boston, Massachusetts 02215, USA

(Received 6 December 2023; accepted 16 July 2024; published 7 August 2024)

Shadow tomography aims to build a classical description of a quantum state from a sequence of simple random measurements. Physical observables are then reconstructed from the resulting classical shadow. Shadow protocols which use single-body random measurements are simple to implement and capture few-body observables efficiently, but do not apply to systems with fundamental number conservation laws, such as ultracold atoms. We address this shortcoming by proposing and analyzing a new local shadow protocol adapted to such systems. The All-Pairs protocol requires one layer of two-body gates and only poly(V) samples to reconstruct arbitrary few body observables. Moreover, by exploiting the permutation symmetry of the protocol, we derive a linear time postprocessing algorithm which applies to both hardcore bosons and spinless fermions in any spatial dimension. We provide a proof-of-principle reference implementation and demonstrate the reconstruction of two- and four-point functions in a paired Luttinger liquid of hardcore bosons.

DOI: 10.1103/PhysRevLett.133.060802

Quantum state tomography aims to produce a complete classical description of the state ρ of a quantum system: a prohibitive task requiring exponentially many measurements of independently prepared copies of ρ. Rather than measure all possible matrix elements, recent works have taken a statistical approach designed to capture classes of observables of physical interest [1–16]. The shadow tomography framework is illustrated in Fig. 1: for each copy of ρ, sample a unitary circuit U from a bespoke ensemble, apply it to ρ, and measure in the computational basis. Physical observables can later be reconstructed by classical postprocessing from the record of applied unitaries and measurement outcomes—the *classical shadow*.

Perhaps the most important shadow protocol is adapted to the efficient reconstruction of few-body observables. The *product* protocol is deceptively simple: each U is a product of independently sampled random 1-body gates [see Fig. 2(a)]. The protocol is efficient by several measures (cf. row 1 of Table I): each measurement requires only a few quantum gates (low *gate complexity*), while the number of classical postprocessing steps scales at most linearly with the number of qubits V (low *classical complexity*). The number of samples required to estimate a few-body observable scales exponentially with the support w of the observable, but is independent of system size (low *sample complexity*). Accordingly, the product protocol has developed into an important experimental tool for characterizing many-qubit systems [17–21].

Many quantum systems, such as ultracold atoms [24–26], are constrained by fundamental symmetries which restrict the available unitary gates as well as the measurement basis. Such restrictions render the simple product protocol tomographically incomplete. As an example, consider an atom living in two sites. The only single-site gates which are consistent with the conservation of atom number are phase operators. These do not affect the statistics of measurements in the occupation basis. Consequently, no product shadow protocol can distinguish the two Bell states $|01\rangle \pm |10\rangle$.

Of course, *two*-body gates are sufficient to rotate the Bell basis into the occupation basis and number-conserving shadow protocols based on global random unitaries and/or

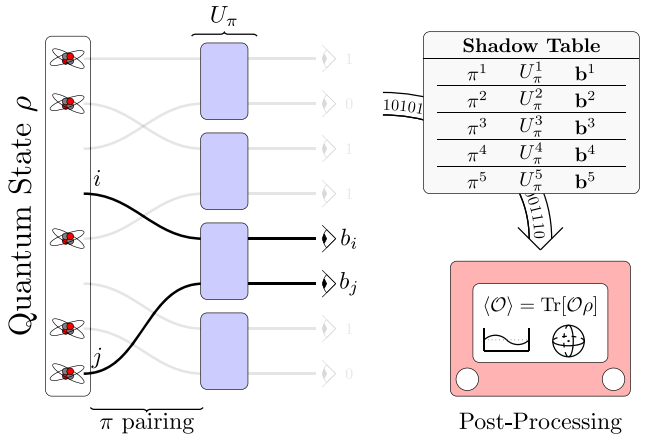

FIG. 1. The All-Pairs shadow protocol: for each copy of the quantum state ρ, (1) randomly choose a pairing π of the V sites and apply swaps to bring paired sites together. The figure shows a swap circuit implementing the pairing $\pi = [1\,3][2\,5][4\,8][6\,7]$. (2) Apply random 2-body number-conserving unitary gates to each pair $[ij]$ in π. (3) Measure in the occupation basis with result $\mathbf{b}$. (4) Record the chosen pairing, gates, and outcomes as a row in the shadow table. Few-body observables can be efficiently reconstructed from the shadow table.

(a)

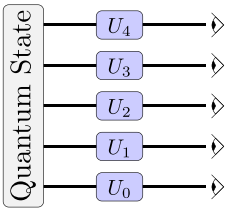

(b)

S_iS_j	$\mathcal{M}_{[ij]}[S_iS_j]$
I_iI_j	I_iI_j
Z_iZ_j	Z_iZ_j
I_iZ_j	$\frac{2}{3}I_iZ_j + \frac{1}{3}Z_iI_j$
Z_iI_j	$\frac{2}{3}Z_iI_j + \frac{1}{3}I_iZ_j$
$a_i^\dagger a_j$	$\frac{1}{3}a_i^\dagger a_j$
$a_i a_j^\dagger$	$\frac{1}{3}a_i a_j^\dagger$
Else	0

FIG. 2. (a) A product protocol of single-body unitaries. (b) The action of $\mathcal{M}_{[ij]}$ defined in Eq. (6) on the operator basis. The channel preserves the number of I, Z, $a^\dagger$, and a operators, but can rescale or swap operators.

deep quantum circuits are generically tomographically complete [3,23,27]. However, as such unitaries scramble local information, these protocols lose any advantage for reconstructing few-body observables: the sample complexity scales exponentially in system size.

In this Letter, we propose a tomographically complete shadow protocol adapted to reconstructing few-body observables in number-conserving systems of fermionic or bosonic hard-core atoms. The All-Pairs protocol is straightforward (see Fig. 1): the random unitaries are constructed by first choosing a random pairing between all sites in the system and then choosing an independent random two-body gate on each pair. It turns out that this shallow but fluctuating circuit geometry permits access to arbitrary few-body observables without scrambling local information. More precisely, the sample complexity scales polynomially with system size V.

Unlike global channels and deep circuits, the All-Pairs protocol has low classical complexity (scaling linearly with V), so that the reconstruction of observables is efficient. This efficiency is a consequence of the permutation symmetry of the protocol, which leads to significant analytic reductions. Table I presents analytically obtained complexity bounds for the All-Pairs protocol, and compares it to other protocols discussed in the literature [3,23,28–30].

We first review key concepts from the shadow tomography formalism. Using this formalism, we express the All-Pairs protocol as a quantum channel and analyze its decomposition into symmetry sectors. The eigenvalues and eigenoperators of the channel bound the classical and sample complexity for the protocol. Finally, as a proof-of-concept, we reconstruct two- and four-point functions in a bosonic model with a paired Luttinger liquid ground state.

Background and notation—We adopt the shadow tomography formalism developed in Ref. [3]. The *shadow channel* describes the action of the shadow measurement protocol,

$$\mathcal{M}[\rho] = \int dU \sum_{\boldsymbol{b}} \mathrm{Tr}[\rho(U^\dagger|\boldsymbol{b}\rangle\langle\boldsymbol{b}|U)](U^\dagger|\boldsymbol{b}\rangle\langle\boldsymbol{b}|U) \equiv \mathop{\mathbb{E}}_{U,\boldsymbol{b}}[U^\dagger|\boldsymbol{b}\rangle\langle\boldsymbol{b}|U], \tag{1}$$

on a quantum state ρ. Here, U is the randomly sampled unitary and $|\boldsymbol{b}\rangle$ is the postmeasurement basis state. The shadow protocol is tomographically complete if and only if the channel is invertible, in which case

$$\rho = \mathop{\mathbb{E}}_{U,\boldsymbol{b}}[\mathcal{M}^{-1}[U^\dagger|\boldsymbol{b}\rangle\langle\boldsymbol{b}|U]]. \tag{2}$$

The shadow table T is the set of independently sampled U and obtained measurement outcomes $\boldsymbol{b}$. An unbiased estimator $\hat{\rho}$ for ρ is constructed by replacing the $\mathbb{E}$ in Eq. (2) with an empirical average over the entries in T. The application of $\mathcal{M}^{-1}$ is done classically, so that the difficulty of the inversion determines the postprocessing complexity.

Given the inverse channel, estimating the expectation of an operator $\langle O\rangle$ from a measurement record is straightforward,

$$\widehat{\langle O\rangle} = \mathrm{Tr}[\hat{\rho}O] = \frac{1}{|T|}\sum_{(U,\boldsymbol{b})\in T}\mathrm{Tr}[(U^\dagger|\boldsymbol{b}\rangle\langle\boldsymbol{b}|U)\mathcal{M}^{-1}[O]]. \tag{3}$$

Here, we have used the Hermiticity of $\mathcal{M}^{-1}$ with respect to the trace inner product. Clearly, the number of samples in T and the variance of the underlying distribution determine the statistical error on the estimate of the expectation value. The number of samples required to obtain a fixed standard error is controlled by the *shadow norm* of the operator O [31],

TABLE I. Resource complexity for estimating the expectation value of w-body operator strings allowing long range few-body operators. The ergodic protocol has a sample complexity which depends on the native Hamiltonian and evolution time.

Protocol	U(1) Compatible	Gate complexity	Classical complexity		Sample complexity
			One-time	Per sample	
Product [3]	No	V		w	3^w
Global random circuit [3]	Yes	V^2 [22]		$V^2 2^V$	2^V
Ergodic evolution [23][23]	Yes	Hamiltonian	$(2^{2V})^3$	2^{2V}	$\geq 2^V$
All-pairs	Yes	$(V/2)$	$(n_z)^3$	$V + n_z 2^{2n_z}$	$(\frac{3}{2})^{n_+ + 2n_z} \times (V^{n_+}/n_+!)$

$$\|O\|_s^2 = \max_{\rho:\ \text{state}} \mathop{\mathbb{E}}_{U,\boldsymbol{b}} |\mathrm{Tr}[(U^\dagger|\boldsymbol{b}\rangle\langle\boldsymbol{b}|U)\mathcal{M}^{-1}[O]]|^2. \quad (4)$$

The rhs is maximized over density matrices ρ, and as noted in [3], only the traceless components of O contribute to the shadow norm. In practice, one employs *median-of-means* estimation to reduce the probability of large errors [3].

Although the protocol applies to fermions as well, we focus on a system of conserved hard-core bosons on V sites and adopt a local operator basis adapted to number conservation, $S \in \{I, Z, a^\dagger, a\}^{\otimes V}$ where $a^\dagger = \frac{1}{2}(X - iY)$ and $a = \frac{1}{2}(X + iY)$ are the usual raising and lowering operators for a two-level system, with the $|\uparrow\rangle$ state identified as the empty state. Number-conserving strings are those in which $a^\dagger$ and a appear in equal number. The number of $a^\dagger$ or a operators in a basis string is denoted by n_+, and the number of Z operators by n_z. It is straightforward to confirm these strings form an orthogonal basis for all number-conserving operators on a V-site system (Supplemental Material, Sec. Ia [32]).

The All-Pairs channel—We now apply the shadow formalism to the All-Pairs protocol. The channel is an average over pairings π from the set of all possible pairings of sites P_V,

$$\mathcal{M} = \frac{1}{|P_V|} \sum_{\pi \in P_V} \mathcal{M}_\pi. \quad (5)$$

Each pairing π is a grouping of the V sites into $V/2$ pairs. The number of such pairings is $|P_V| = (V-1)!!$. For odd V a single site is left out of any given pairing and $|P_V| = V(V-2)!!$. Each pair of sites $[ij] \in \pi$ is acted on by two-body unitaries, resulting in a product channel

$$\mathcal{M}_\pi = \prod_{[ij]\in\pi} \mathcal{M}_{[ij]},$$
$$\mathcal{M}_{[ij]}[\rho] = \mathop{\mathbb{E}}_{U_{[ij]}, b_i b_j} \left[U_{[ij]}^\dagger |b_i b_j\rangle\langle b_i b_j| U_{[ij]} \right]. \quad (6)$$

Sampling $U_{[ij]}$ from an ensemble which forms a 2-design over the number-conserving unitary group [22,33–35], $\mathcal{M}_{[ij]}$ can be evaluated block by block,

$$\mathcal{M}_{[ij]}\left[\begin{pmatrix} \rho_0 & & \\ & \rho_1 & \\ & & \rho_2 \end{pmatrix}\right] = \begin{pmatrix} \rho_0 & & \\ & \frac{1}{3}(\rho_1 + I_{2\times 2}\mathrm{Tr}\rho_1) & \\ & & \rho_2 \end{pmatrix}. \quad (7)$$

Here, ρ_0 and ρ_2 are scalars representing the $m = 0$ and $m = 2$ number sectors, whereas ρ_1 is a 2×2 matrix describing states $|01\rangle$ and $|10\rangle$ in the occupation basis. Expanding Eq. (7) in the basis of operator strings yields the table in Fig. 2(b).

Analysis of the channel—It is straightforward to show that the All-Pairs channel is tomographically complete. Consider an operator string S we wish to reconstruct using the information in the shadow table T. Begin by filtering T down to only those rows whose pairings match $a^\dagger$ with a and Z with another Z operator within S; call this filtered channel $\mathcal{M}_S$. It is clear from Fig. 2(b) that the action of this effective channel is diagonal on S and inversion is trivial $\mathcal{M}_S^{-1}[S] = 3^{n_+} S$. The choice of S is arbitrary so all operators can be reconstructed from the information contained in T. However, the process described above is inefficient and throws out most entries of the table. To make the protocol more efficient and greatly reduce its sample complexity we now diagonalize the channel without prior filtering.

The All-Pairs channel can be efficiently diagonalized and inverted due to strong symmetry constraints. First, $\mathcal{M}$ is manifestly permutation symmetric. For any permutation σ of the V sites,

$$\mathcal{M}[\sigma S \sigma^\dagger] = \sigma \mathcal{M}[S] \sigma^\dagger. \quad (8)$$

Second, $\mathcal{M}$ conserves the number of I, Z, a, and $a^\dagger$ operators in an operator string S. Third, $a^\dagger$ and a operators are immobile under the action of $\mathcal{M}$ [cf. Fig. 2(b)].

Consider an operator string with n_+ instances of a and $a^\dagger$ and n_z instances of Z in a canonically ordered form, $S_\circ = (a^\dagger \otimes a)^{\otimes n_+} \otimes Z^{\otimes n_z} \otimes I^{\otimes V-w}$. Since $\mathcal{M}_\pi[S_\circ]$ vanishes unless π pairs the a and $a^\dagger$ operators, the channel action factorizes

$$\mathcal{M}[S_\circ] = \frac{f}{3^{n_+}} (a^\dagger \otimes a)^{\otimes n_+} \otimes \mathcal{M}[Z^{\otimes n_z} \otimes I^{\otimes V-w}]. \quad (9)$$

Here, f denotes the fraction of pairings which contribute,

$$f = n_+! \frac{|P_{(V-2n_+)}|}{|P_V|}. \quad (10)$$

We now focus on the action of $\mathcal{M}$ restricted to the space of operators spanned by $S \in \{I, Z\}^{\otimes V}$. Since $\mathcal{M}$ conserves the number of Z's, it defines a permutation-symmetric hard-core random walk of the Z's (formally, a symmetric exclusion process). Accordingly, the channel decomposes into Z sectors, labeled by n_z, and irreducible representations of the permutation group, labeled by $\lambda = (V - \lambda_2, \lambda_2)$. Each n_z, λ irrep appears once and has a corresponding eigenvalue c_λ which is independent of n_z.

We use combinatorial arguments to derive closed but rather long expressions for the eigenvalues c_λ in Supplemental Material, Sec. IIc [32]. This decomposition underlies the computationally efficient inversion scheme and the rigorous bounds on the sample complexity.

Inverting the channel—To compute the estimator Eq. (3) from the shadow table, we need an efficient algorithm to apply the inverse channel $\mathcal{M}^{-1}$ to string operators within the trace. The description of the reconstruction algorithm is

presented in Supplemental Material, Sec. II [32]. Here, we sketch the key steps which reduce the problem to inverting an $(n_z+1)\times(n_z+1)$ matrix.

With reference to Eq. (9), the nontrivial part of inverting $\mathcal{M}$ comes from its action on strings $S\in\{I,Z\}^{\otimes V}$. Permutation symmetry and n_z conservation impose that

$$\mathcal{M}[S_\circ]=\sum_{d=0}^{n_z}\alpha_d\sum_{\substack{S_d \text{ at}\\ \text{distance } d}} S_d, \tag{11}$$

where the strings S_d are at swap distance d from the reference string $S_\circ$. Using (5), it is possible to obtain the amplitudes α_d in closed form (Supplemental Material, Sec. IIb [32]).

The two decompositions, into c_λ and into α_d, linearly parametrize the channel $\mathcal{M}$ in a given n_z sector. Thus, there is a linear relationship,

$$c_\lambda=\sum_{d=0}^{n_z}G_{\lambda d}\alpha_d, \tag{12}$$

where G is an $(n_z+1)\times(n_z+1)$ integer matrix determined entirely by the symmetry of the channel. We use combinatorial arguments to obtain G in closed form in Supplemental Material, Sec. IIc [32].

The inverse channel is simple in terms of its irrep decomposition, its eigenvalues are simply $(1/c_\lambda)$. In order to efficiently apply $\mathcal{M}^{-1}$ to a string S, we need the amplitudes β_d which govern how it delocalizes S to other strings with swap distance d. These can be obtained using the inverse of Eq. (12). Schematically, we perform the following steps,

$$\mathcal{M}\to\alpha_d\xrightarrow{G}c_\lambda\xrightarrow{\text{invert}}\frac{1}{c_\lambda}\xrightarrow{G^{-1}}\beta_d\to\mathcal{M}^{-1}.$$

Equation (3) thus becomes

$$\mathrm{Tr}[\hat{\rho}S_\circ]=\frac{1}{|T|}\sum_{(U,\boldsymbol{b})\in T}\sum_{d}^{n_z}\beta_d\mathrm{Tr}\left[U^\dagger|\boldsymbol{b}\rangle\langle\boldsymbol{b}|U\sum_{\substack{S \text{ at}\\ \text{distance } d}} S\right]. \tag{13}$$

Naively, there are $\binom{V}{n_z}$ terms in this decomposition, each of which takes $\mathcal{O}(n_z)$ time to evaluate. However, the expectation values of uniformly delocalized $\{I,Z\}$ strings depend only on the measurement string $\boldsymbol{b}$ and not the particular choice of two-body gates $U_{[ij]}$. To compute (13), we only need to read the measurement result in $\mathcal{O}(V)$ time, then perform a sum over $\mathcal{O}(4^{n_z})$ strings, calculating the trace for each. The details of this algorithm are provided in Supplemental Material, Sec. IIe, and pseudocode for implementing the fast expectation value calculation are provided in Supplemental Material, Sec. IIf [32].

Sample complexity—The shadow-norm (4) bounds the sample complexity of the All-Pairs channel. For the same reasons which lead to the factorization in (9), the shadow norm can be separately evaluated for operator strings of $a^\dagger$ and a, and strings of I and Z. The latter is bounded using the eigenvalues c_λ. For $V\gg n_z\geq\lambda_2$, which is the relevant limit for reconstruction of low weight operators in large systems, the eigenvalues of $\mathcal{M}^{-1}$ scale as $c_\lambda^{-1}\simeq(3/2)^{\lambda_2}-\mathcal{O}(V^{-1})$. Accounting for the a, $a^\dagger$ pairs (Supplemental Material, Sec. III [32]) one obtains

$$\|S\|_{\mathrm{s}}^2\leq\left(\frac{3}{2}\right)^{n_++2n_z}\left(\frac{V^{n_+}}{n_+!}\right)\|S\|_\infty^2. \tag{14}$$

Notably, the shadow norm acquires a polynomial volume dependence compared to the single-unitary product channel without conserved charges, and retains a similar exponential dependence on the weight.

Experimental considerations—The essential experimental requirements to implement the All-Pairs protocol are (1) the ability to shuttle sites to bring paired sites into adjacency; (2) application of two-body gates to selected neighboring pairs; and (3) single-site occupation measurement. Although our analysis above has assumed that the two-body gates are Haar random, it turns out that much simpler gate sets suffice. For example, a uniform ensemble on the three gates

$$G=\{I,\sqrt{\mathrm{iSWAP}},\sqrt{\mathrm{iSWAP}}\times(S\otimes I)\} \tag{15}$$

suffices. Here, S is the phase gate and $\sqrt{\mathrm{iSWAP}}$ corresponds to a 50-50 beam splitter.

Demonstration with paired Luttinger liquid—To demonstrate the utility of the All-Pairs channel, we illustrate its application to a system of hard-core bosons on a two-leg ladder which can be tuned to be a paired or unpaired Luttinger liquid. This example shows that the All-Pairs channel can be used to estimate arbitrary number-conserving correlation functions; it is *not* limited to two-point functions.

We label the bosons a and b on the top and bottom rails of a ladder with Hamiltonian $H=H_{\mathrm{hop}}+H_{\mathrm{int}}$, where

$$\begin{aligned}H_{\mathrm{hop}}&=-t\sum_i\left[a_i^\dagger a_{i+1}+b_i^\dagger b_{i+1}+a_i^\dagger b_i\right]+\mathrm{H.c.},\\ H_{\mathrm{int}}&=-U\sum_i a_i^\dagger a_i b_i^\dagger b_i.\end{aligned} \tag{16}$$

The interaction term H_{int} is an attractive density-density interaction across rungs of the ladder.

In the limit $t\gg U$, the bosons form a Luttinger liquid in which correlations of a single boson species decay as a power law, $\langle a_i^\dagger a_j\rangle\sim|i-j|^{-\alpha}$. When the interaction dominates, $t\ll U$, the bosons form "molecules" across rungs,

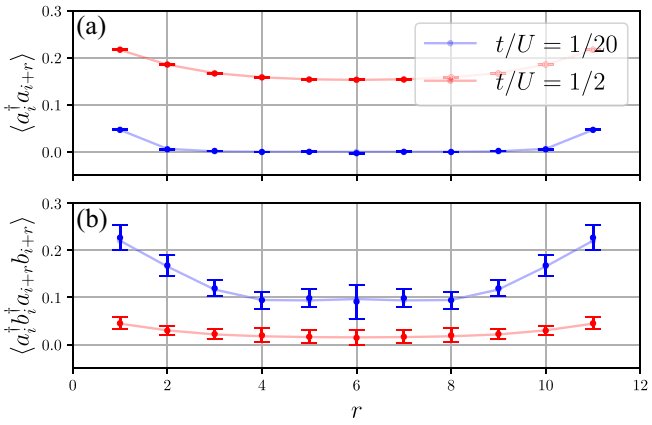

FIG. 3. Two- and four-body correlation functions in a system of hardcore bosons on a two-leg ladder. The system realizes a paired or unpaired Luttinger liquid in the blue or red data. All-Pairs protocol estimates (markers) reconstructs correlation functions of the ground state (solid lines). We show the average and standard deviation of 50 independent shadow tables with $N = 2 \times 10^4$ samples each.

which then condense into a paired liquid. Here, the single-species correlators vanish exponentially, while pair correlations of the form $\langle a_i^\dagger b_i^\dagger a_j b_j \rangle$ exhibit power laws.

We use the All-Pairs protocol to estimate single-boson and pair correlation functions in the ground state of H obtained through exact diagonalization. We consider a ladder with 12 rungs ($V = 24$ sites) at $1/4$ filling with periodic boundary conditions. Following Eq. (14), we use $N \sim 2 \times 10^4$ samples to get a bound on $\varepsilon \sim 1/5$ standard error on four-body operators, although in practice the realized error is significantly smaller [36]. We construct 50 independent shadow tables to demonstrate that the empirical average estimator is unbiased and has small variance (cf. Fig 3). We note that the primary computational bottleneck in this exercise comes from acquiring the data, not the reconstruction itself; that is, most resources are consumed by exact diagonalization and sampling of the ground state.

Outlook—We have demonstrated that the All-Pairs protocol provides efficient local shadow tomography in systems with fundamental number conservation. Thus, our protocol enables the tomographic investigation of strongly correlated many-body states in quantum simulators. While we restricted to hard-core bosons in the main text, our results apply *mutatis mutandis* to fermions (Supplemental Material, Sec. IIf [32]).

Our algorithm for channel inversion allows for the estimation of w-body number-conserving correlation functions with resource requirements that scale favorably in comparison with alternative protocols (see Table I). Previous work has focused on Hamiltonian evolution [5,23,30], which may be more practical to implement on some devices but requires an extremely accurate model of the underlying Hamiltonian in addition to significant classical postprocessing resources.

Compared to systems without fundamental number conservation, the sample complexity has gained a volume dependence $\mathcal{O}(V^{n_+})$. We believe this volume scaling is optimal for estimating local observables. In certain regimes shallow circuits can improve sample complexity in systems without number conservation [38–40], but it is unclear whether these improvements translate to systems with conservation laws.

There are two natural generalizations. Allowing internal states, the All-Pairs protocol generalizes by taking the two-body gates to be Haar on the local space. Allowing multiple occupancy ($M > 1$ particles per site), one must extend to the "All-Tuples" protocol, in which the random pairings are replaced by random $(2M-1)$-tuples. In both of these cases, it is clear the channel remains tomographically complete and permutation symmetric. We leave the analysis of the reconstruction algorithm and sample complexity to future work.

Acknowledgments—This work was supported by the Air Force Office of Scientific Research through Grant No. FA9550-16-1-0334 (M. O. F.) and by the National Science Foundation through the Grants No. DMR-1752759 (S. N. H., M. O. F., and A. C.) and No. PHY-1752727 (C. R. L.).

[1] S. Aaronson, in *Proceedings of the 50th Annual ACM SIGACT Symposium on Theory of Computing, STOC 2018* (Association for Computing Machinery, New York, 2018), pp. 325–338.
[2] S. Aaronson and G. N. Rothblum, in *Proceedings of the 51st Annual ACM SIGACT Symposium on Theory of Computing, STOC 2019* (Association for Computing Machinery, New York, 2019), pp. 322–333.
[3] H.-Y. Huang, R. Kueng, and J. Preskill, Nat. Phys. **16**, 1050 (2020).
[4] S. Shivam, C. W. von Keyserlingk, and S. L. Sondhi, SciPost Phys. **14**, 094 (2023).
[5] Z. Liu, Z. Hao, and H.-Y. Hu, arXiv:2311.00695.
[6] S. Chen, W. Yu, P. Zeng, and S. T. Flammia, PRX Quantum **2**, 030348 (2021).
[7] A. Zhao, N. C. Rubin, and A. Miyake, Phys. Rev. Lett. **127**, 110504 (2021).
[8] D. E. Koh and S. Grewal, Quantum **6**, 776 (2022).
[9] C. Kokail, R. van Bijnen, A. Elben, B. Vermersch, and P. Zoller, Nat. Phys. **17**, 936 (2021).
[10] R. J. Garcia, Y. Zhou, and A. Jaffe, Phys. Rev. Res. **3**, 033155 (2021).
[11] Y. Zhan, A. Elben, H.-Y. Huang, and Y. Tong, arXiv:2309.00774.
[12] C. Hadfield, S. Bravyi, R. Raymond, and A. Mezzacapo, arXiv:2006.15788.
[13] R. Levy, D. Luo, and B. K. Clark, Phys. Rev. Res. **6**, 013029 (2024).

[14] S. H. Sack, R. A. Medina, A. A. Michailidis, R. Kueng, and M. Serbyn, PRX Quantum **3**, 020365 (2022).
[15] T.-G. Zhou and P. Zhang, arXiv.2309.01258.
[16] S. J. Garratt and E. Altman, PRX Quantum **5**, 030311 (2024).
[17] S. J. van Enk and C. W. J. Beenakker, Phys. Rev. Lett. **108**, 110503 (2012).
[18] T. Brydges, A. Elben, P. Jurcevic, B. Vermersch, C. Maier, B. P. Lanyon, P. Zoller, R. Blatt, and C. F. Roos, Science **364**, 260 (2019).
[19] A. Elben, B. Vermersch, C. F. Roos, and P. Zoller, Phys. Rev. A **99**, 052323 (2019).
[20] A. Elben, S. T. Flammia, H.-Y. Huang, R. Kueng, J. Preskill, B. Vermersch, and P. Zoller, Nat. Rev. Phys. **5**, 9 (2022).
[21] M. Ippoliti, Quantum **8**, 1293 (2024).
[22] S. N. Hearth, M. O. Flynn, A. Chandran, and C. R. Laumann, arXiv.2306.01035.
[23] M. C. Tran, D. K. Mark, W. W. Ho, and S. Choi, Phys. Rev. X **13**, 011049 (2023).
[24] H. Ritsch, P. Domokos, F. Brennecke, and T. Esslinger, Rev. Mod. Phys. **85**, 553 (2013).
[25] I. Bloch, J. Dalibard, and W. Zwerger, Rev. Mod. Phys. **80**, 885 (2008).
[26] A. M. Kaufman, B. J. Lester, C. M. Reynolds, M. L. Wall, M. Foss-Feig, K. R. A. Hazzard, A. M. Rey, and C. A. Regal, Science **345**, 306 (2014).
[27] J. Bringewatt, J. Kunjummen, and N. Mueller, Quantum **8**, 1300 (2024).
[28] H.-Y. Hu, S. Choi, and Y.-Z. You, Phys. Rev. Res. **5**, 023027 (2023).
[29] G. H. Low, arXiv:2208.08964.
[30] D. K. Mark, J. Choi, A. L. Shaw, M. Endres, and S. Choi, Phys. Rev. Lett. **131**, 110601 (2023).
[31] We include an absolute value compared to [3] to account for non-Hermitian operators O. This amounts to controlling the real and imaginary parts of the estimator.
[32] See Supplemental Material at http://link.aps.org/supplemental/10.1103/PhysRevLett.133.060802 for details.
[33] I. Marvian, Nat. Phys. **18**, 283 (2022).
[34] D. Weingarten, J. Math. Phys. (N.Y.) **19**, 999 (1978).
[35] B. Collins, S. Matsymoto, and J. Novak, Not. Am. Math. Soc. **69**, 734 (2022).
[36] In a translationally invariant system, the sample complexity for the full correlation function does not differ significantly from that of a single operator. This can be understood as a special case of the double Dixie Cup problem [37].
[37] D. J. Newman, Am. Math. Mon. **67**, 58 (1960).
[38] A. A. Akhtar, H.-Y. Hu, and Y.-Z. You, Quantum **7**, 1026 (2023).
[39] C. Bertoni, J. Haferkamp, M. Hinsche, M. Ioannou, J. Eisert, and H. Pashayan, Phys. Rev. Lett. **133**, 020602 (2024).
[40] M. Ippoliti, Y. Li, T. Rakovszky, and V. Khemani, Phys. Rev. Lett. **130**, 230403 (2023).